Type II Radio Supernovae and SN 1987A

Kurt W. Weiler & Marcos J. Montes

NRL, Code 7214, Washington, DC 20375-5320; weiler@rsd.nrl.navy.mil & mmontes@moon.nrl.navy.mil

Schuyler D. Van Dyk

Visiting Scientist, Dept. of Physics & Astronomy, UCLA, Los Angeles, CA 90095; vandyk@jean.astro.ucla.edu

Richard A. Sramek

P.O. Box 0, NRAO, Socorro, NM 87801; dsramek@nrao.edu

Nino Panagia

STScI, 3700 San Martin Drive, Baltimore, MD 21218 & Astrophysics Division, Space Science Department of ESA; panagia@stsci.edu

Abstract. Study of radio supernovae over the past 17 years includes two dozen detected objects and almost 80 upper limits. From this work we are able to identify classes of radio properties, demonstrate conformance to and deviations from existing models, estimate the density and structure of the circumstellar material, and by inference the evolution of the presupernova stellar wind, and reveal the last stages of stellar evolution before explosion. It may also be possible to detect thermal hydrogen along the line of sight, to demonstrate binary properties of the stellar system, and to show clumpiness of the circumstellar material. More speculatively, it may be possible to provide distance estimates to radio supernovae. A summary of the radio information can be found at: http://rsd-www.nrl.navy.mil/7214/weiler/sne-home.html.

1. Introduction

A series of papers published over the past 17 years on radio supernovae (RSNe) has established the radio detection and/or radio evolution for 23 objects: 2 Type Ib supernovae, 4 Type Ic supernovae, and 17 Type II supernovae. A much larger list of almost 80 more SNe have low radio upper limits (Table 1).

In this extensive study of the radio emission from SNe, several effects have been noted: 1) Type Ia are not radio emitters to the detection limit of the VLA (The VLA is operated by the NRAO of the AUI under a cooperative agreement with the NSF.); 2) Type Ib/c are radio luminous with steeper spectral indices and a fast turn-on/turn-off, usually peaking at 6 cm near or before optical

Table 1. Observed Supernovae (D = Detection; L = Light Curve)

SN Name	Type	Radio?	SN Name	Type	Radio?	SN Name	Type	Radio?
1940A	II-L		1984E	II-L		1991ar	Ic	
1950B	II?	D	1984L	Ib	L	1991av	IIn	
1957D	II?	D	1984R	?		1991bg	Ia	
1968D	II	D	1985A	Ia		1992A	Ia	
1970A	II?		1985B	Ia		1992H	II-P	
1970G	II-L	L	1985F	Ib		1992ad	II-P?	D
1970L	I?		1985G	II-P		1992bd	II	
1971G	I?		1985H	II		1993G	II	
1971I	Ia		1985L	II-L	D	1993J	IIb	L
1971L	Ia		1986A	Ia		1993N	IIn	
1971R	?		1986E	II-P	L	1993X	II	
1972E	Ia		1986G	Ia		1994D	Ia	
1972T	?		1986I	II-P		1994I	Ic	L
1974E	?		1986J	IIn	L	1994P	II	
1974G	Ia		1986O	Ia		1994W	IIn	
1975N	Ia		1987A	II	L	1994Y	IIn	
1977B	?		1987D	Ia		1994ai	Ic	
1978B	II		1987D	Ia		1994ai	Ic	
1978G	II		1987F	IIpec		1994ak	IIn	
1978K	II	L	1987K	IIb		1995G	IIn	
1979B	Ia		1987M	Ic		1995N	IIn	D
1979C	II-L	L	1987N	Ia		1995X	II-P	
1980I	Ia		1988I	IIn		1995ad	II-P	
1980K	II-L	L	1988Z	IIn	L	1995al	Ia	
1980L	?		1989B	Ia		1996N	Ic	D
1980N	Ia		1989C	IIn		1996W	IIp	
1980O	II		1989L	II-L		1996X	Ia	
1981A	II		1989M	Ia		1996ae	IIn	
1981B	Ia		1989R	IIn		1996an	II	
1981K	II?	L	1990B	Ic	L	1996aq	Ic	
1982E	Ia?		1990K	II-L		1996bu	IIn	
1982R	Ib?		1990M	Ia		1996cb	IIb?	D
1983K	II-P		1991T	Ia		1997X	Ic	D
1983N	Ib	L	1991ae	IIn				

maximum; and 3) Type II show a range of radio luminosities with flatter spectral indices and a relatively slow turn-on/turn-off.

2. Models

All known RSNe appear to share common properties of: 1) non-thermal synchrotron emission with high brightness temperature; 2) a decrease in absorption with time, resulting in a smooth, rapid turn-on first at shorter wavelengths and later at longer wavelengths; 3) a power-law decline of the flux density with time at each wavelength after maximum flux density (optical depth ≈ 1) is reached at that wavelength; and 4) a final, asymptotic approach of spectral index α to an optically thin, non-thermal, constant negative value (Weiler et al. 1986, 1990). Chevalier (1982a,b) has proposed that the relativistic electrons and enhanced magnetic field necessary for synchrotron emission arise from the SN shock interacting with a relatively high-density circumstellar medium (CSM) which has been ionized and heated by the initial UV/X-ray flash. This CSM is presumed to have been established by a constant mass-loss ($\dot{M}$) rate, constant velocity

(w) wind (i.e., $\rho \propto r^{-2}$) from a red supergiant (RSG) progenitor or companion. This CSM is also the source of the initial absorption.

2.1. Parameterized Radio Light Curves

The parameterized model of Weiler et al. (1986, 1990) and Montes et al. (1997) may be written as

$$S(\mathrm{mJy}) = \mathrm{K}_1 \left(\frac{\nu}{5\ \mathrm{GHz}}\right)^{\alpha} \left(\frac{\mathrm{t}-\mathrm{t}_0}{1\ \mathrm{day}}\right)^{\beta} \mathrm{e}^{-(\tau+\tau'')} \left(\frac{1-\mathrm{e}^{-\tau'}}{\tau'}\right), \quad (1)$$

where

$$\tau = K_2 \left(\frac{\nu}{5\ \mathrm{GHz}}\right)^{-2.1} \left(\frac{t-t_0}{1\ \mathrm{day}}\right)^{\delta}, \quad (2)$$

$$\tau' = K_3 \left(\frac{\nu}{5\ \mathrm{GHz}}\right)^{-2.1} \left(\frac{t-t_0}{1\ \mathrm{day}}\right)^{\delta'}, \quad (3)$$

and

$$\tau'' = K_4 \left(\frac{\nu}{5\ \mathrm{GHz}}\right)^{-2.1}. \quad (4)$$

K_1, K_2, and K_3 correspond, formally, to the unabsorbed flux density (K_1), and the uniform (K_2) and non-uniform (K_3) optical depths in the surrounding CSM at 5 GHz one day after the explosion date t_0. K_4 represents a non-time dependent HII absorption ($EM = 8.93 \times 10^7\ K_4\ (T_e/10^4\mathrm{K})^{1.35}$ pc cm^{-6}; Equation 1–223 of Lang 1986) along the line-of-sight to the radio emitting region. The term $e^{-\tau}$ describes the attenuation of a local medium with optical depth τ and time dependence δ that uniformly covers the emitting source ("uniform external absorption"); the term $(1-e^{-\tau'})\tau'^{-1}$ describes the attenuation produced by an inhomogeneous medium with optical depths distributed between 0 and τ' ("clumpy absorption") and time dependence δ'; and the term $e^{-\tau''}$ describes an absorption along the line-of-sight which is constant with time. All absorbing media are assumed to be purely thermal, ionized hydrogen with opacity $\propto \nu^{-2.1}$.

3. Results

The success of the basic parameterization and model description can be seen in the relatively good correspondence between the model fits and the data for the three subtypes of RSNe: Type Ib SN 1983N (Fig. 1), Type Ic SN 1990B (Fig. 1), and Type II SN 1980K (Fig. 2). (N.B. After day $\sim$ 4000, the evolution of the radio emission from SN 1980K deviates from the expected model evolution. See § 8 for discussion of this change.)

4. Mass Loss Rate & Change in Mass Loss Rate

From the Chevalier (1982a,b) model, the turn-on of the radio emission for RSNe provides a measure of the presupernova mass loss rate to wind velocity ratio. Using the formulation of Weiler et al. (1986) Eq. 16, we can write

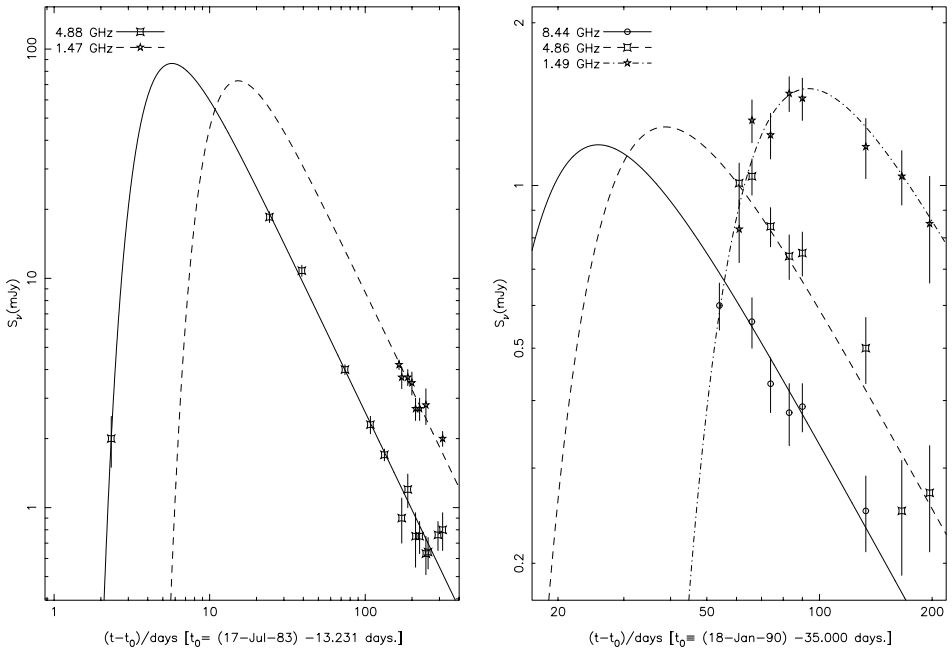

Figure 1. Type Ib SN 1983N (left) at 6 cm (4.9 GHz; *squares, solid line*) and 20 cm (1.5 GHz; *stars, dashed line*) and Type Ic SN 1990B (right) at 3.4 cm (8.4 GHz; *circles, solid line*), 6 cm (4.9 GHz; *squares, dashed line*), and 20 cm (1.5 GHz; *stars, dash-dot line*).

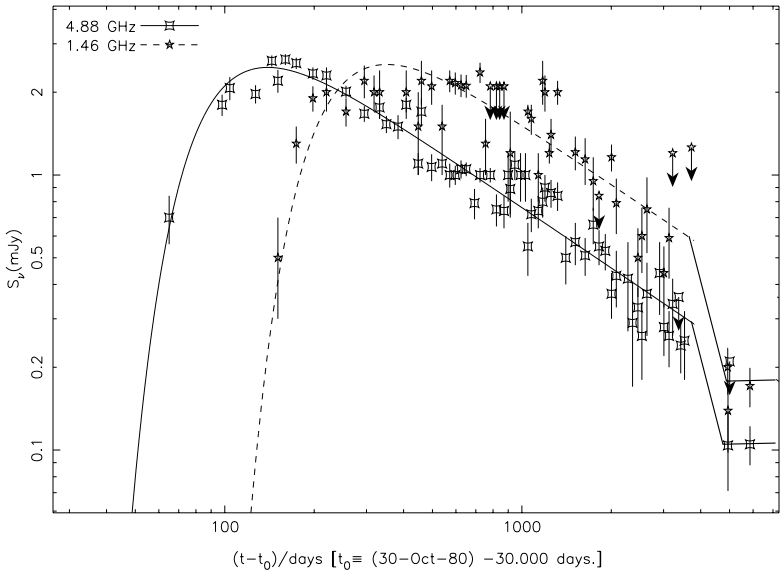

Figure 2. Type II SN 1980K at 6 cm (4.9 GHz; *squares, solid line*), and 20 cm (1.5 GHz; *stars, dashed line*). (For discussion of the sharp drop in flux density after day $\sim$ 4000 see § 8.)

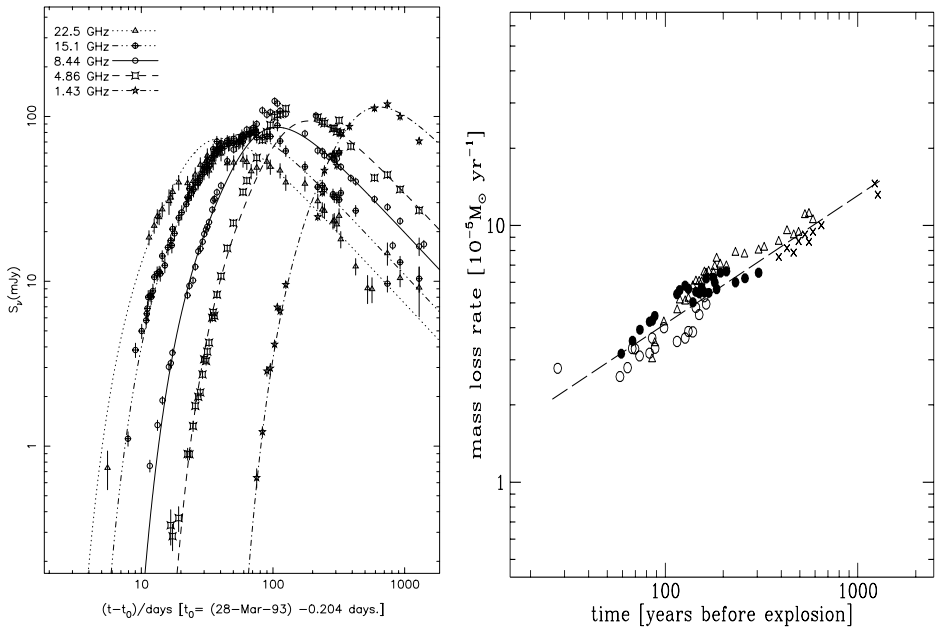

Figure 3. Type II SN 1993J (left) at 1.2 cm (22.5 GHz; *triangles, dotted line*), 2 cm (15.1 GHz; *crossed circles, dash-triple dot line*), 3.4 cm (8.4 GHz; *circles, solid line*), 6 cm (4.9 GHz; *squares, dashed line*), and 20 cm (1.5 GHz; *stars, dash-single dot line*) and mass loss rate (right) of the presumed red supergiant progenitor to SN 1993J vs. time before the explosion.

$$\frac{\dot{M}(M_\odot \text{ yr}^{-1})}{(w/10 \text{ km s}^{-1})} = 3{\times}10^{-6}\, K_2\, m^{-1.5} \left(\frac{v_i}{10^4 \text{ km s}^{-1}}\right)^{1.5} \left(\frac{1}{45 \text{ days}}\right)^{1.5m} \left(\frac{T}{10^4 \text{ K}}\right)^{0.68} \quad (5)$$

where $\dot{M}$ is the presupernova mass loss rate, w is the presupernova wind velocity, K_2 is the same as in Eq. 2, m is the SN shock deceleration index (shock radius $\propto$ t$^{\rm m}$), v_i is the initial SN shock velocity ($\sim$ 13,000 km s^{-1}), and T is the temperature of the circumstellar material ($\sim$ 20,000 K).

From Eq. 5 the mass loss rates from SN progenitors are generally estimated to be $\sim 10^{-6} M_\odot$ yr^{-1} for Type Ib/c SNe and $\sim 10^{-4} M_\odot$ yr^{-1} for Type II SNe. For the specific case of SN1993J, where detailed radio observations are available starting only a few days after explosion (Fig. 3), Van Dyk et al. (1994) find evidence for a changing mass loss rate (Fig. 3) for the presupernova star which was as high as $\sim 10^{-4}\ M_\odot$ yr^{-1} approximately 1000 years before explosion and decreased to $\sim 10^{-5}\ M_\odot$ yr^{-1} just before explosion.

5. Clumpiness of the Presupernova Wind

In their study of the radio emission from SN1986J, Weiler et al. (1990) found that the simple Chevalier (1982a,b) model could not describe the relatively slow turn-on. They therefore added terms described mathematically by τ' in Eqs. 1 and 3. This extension greatly improved the quality of the fit and was interpreted by Weiler et al. (1990) to represent the possible presence of filamentation or clumpiness in the CSM.

Such a clumpiness in the wind material was again required for modelling the radio data from SN1988Z (Van Dyk et al. 1993) and SN1993J (Van Dyk et al. 1994). Evidence for filamentation in the envelopes of SNe has also been found from optical and UV observations (Filippenko et al. 1994, Spyromilio 1994).

6. Binary Systems

In the process of analyzing a full decade of radio measurements from SN 1979C, Weiler et al. (1991, 1992a) found evidence for a significant, quasi-periodic, variation in the amplitude of the radio emission at all wavelengths of $\sim$ 15 % with a period of 1575 days or $\sim$ 4.3 years (see Fig. 4 at age $<$ 4000 days). They interpreted the variation as due to a minor ($\sim$ 8 %) density modulation, with a period of $\sim$ 4000 years, on the larger, relatively constant presupernova stellar mass loss rate. Since such a long period is inconsistent with most models for stellar pulsations, they concluded that the modulation may be produced by interaction of a binary companion in an eccentric orbit with the stellar wind from the presupernova RSG.

Since that time, the presence of binary companions has been suggested for the progenitors of SN1993J (Podsiadlowski et al. 1993) and SN1994I (Nomoto et al. 1994) indicating that binaries may be common in presupernova systems.

7. HII Along the Line-of-Sight

A reanalysis of the radio data for SN 1978K from Ryder et al. (1993) clearly shows flux density evolution characteristic of normal Type II SNe. Additionally, the data indicate the need for a time-independent, free-free absorption component along the line-of-sight. Montes et al. (1997 and elsewhere in this volume) interpret this constant absorption term as indicative of the presence of an HII region along the line-of-sight to SN 1978K, perhaps a part of an HII region associated with the SN progenitor.

8. The Changing Evolution of SN 1979C and SN 1980K

Radio emission that preserves its spectral index while deviating from the parameterized model most likely indicates a change in the average circumstellar density with respect to the expected $\rho \propto r^{-2}$ law.

SN 1979C prior to 1990 (age $<$ 4000 days) follows a standard, albeit sinusoidally modulated (see §6) declining radio emission (see Weiler et al. 1991). However, after $\sim$ 4000 days a slow increase in the radio light curve occurs at all

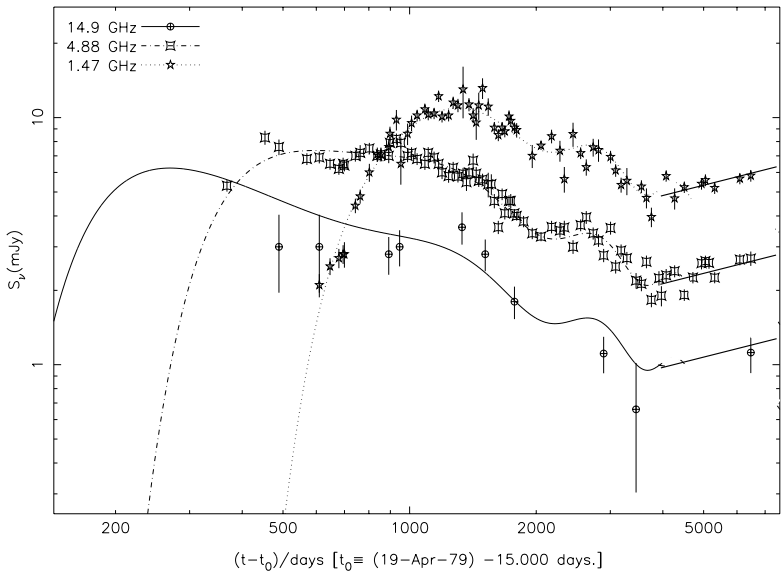

Figure 4. Type II SN 1979C at 2 cm (14.9 GHz; *crossed circles, solid line*), 6 cm (4.9 GHz; *squares, dash-dot line*), and 20 cm (1.5 GHz; *stars, dotted line*).

wavelengths (Fig. 4). By day $\sim$ 6500, this change in evolution implies an *increase* in flux density by a factor of $\sim$ 1.8 with respect to the standard model or a density enhancement by a factor of $\sim$ 1.35. This may possibly be understood as a change of the CSM density profile from the r^{-2} law, which was applicable until day $\sim$ 4000, to an appreciably flatter behavior ($\sim r^{-1.2}$).

SN 1980K prior to day $\sim$ 4000 is also well behaved (Weiler et al. 1992b). However, more recent measurements show a steep *decline* in flux density at all wavelengths by a factor of $\sim$ 2 occurring between day $\sim$ 4000 and day $\sim$ 4500 (Fig. 2). Such a sharp decline in flux density implies a decrease in $\rho_{\rm CSM}$ by a factor of $\sim$ 1.6.

Thus, for both SN 1979C and SN 1980K we have significant changes in radio flux density occurring $\sim$ 4000 days ($\sim$ 10 years) after the explosion. Since the SN shock is moving $\sim$ 1000 times faster than the wind material of the RSG progenitor ($\sim$ 10,000 km s^{-1} vs. $\sim$ 10 km s^{-1}), such a time interval implies a significant change in the presupernova stellar wind properties $\sim$ 10,000 years before the explosion. Although short compared to the lifetimes of typical RSN progenitors, such an interval is comparable to the evolutionary time since the last "blue loop" episode for stars with masses up to $\sim 12 - 14\ M_\odot$ for solar metallicity (and higher for lower metallicities; see Brocato & Castellani 1993, Langer & Maeder 1995) so that changes in the radio emission may indicate a significant transition in the evolution of the presupernova stars.

It is interesting to note that SN 1987A, which exploded as a blue supergiant (BSG), ended a RSG phase a few thousand years earlier. Its initial radio emission (Turtle et al. 1987) declined to a low plateau within a year but began increasing

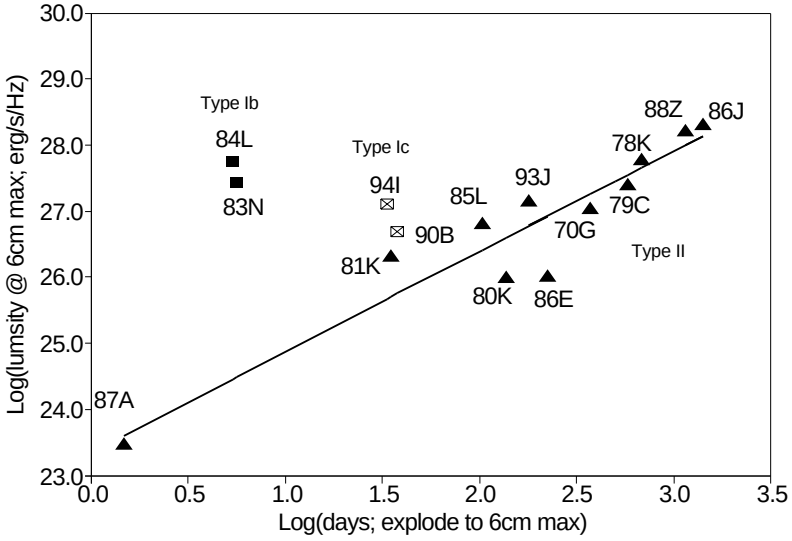

Figure 5. Peak 6 cm luminosity of RSNe vs. time delay, in days, from explosion to peak 6 cm flux density. Type Ib SNe are plotted as *filled squares* and Type Ic as *crossed squares*. Type II SNe are plotted as *filled triangles*. The *solid line* is the best fit to the available Type II RSNe.

again at an age of ~ 3 years and continues to increase at the present time (see Ball et al. 1995, Gaensler et al. 1997, and the presentations by Turtle et al. and Gaensler et al. elsewhere in this volume). Apparently, presupernova stars can undergo significant and rapid changes of state in the last few thousand years before explosion.

9. Peak Radio Luminosities and Distances

If one plots the peak 6 cm radio luminosity for each RSN against the time required after explosion to reach that peak, an interesting phenomenon is apparent: 1) Type Ib/c SNe may have relatively little variation in their peak 6 cm luminosities, even if there are differences in the time from explosion to that peak, and 2) the longer it takes a Type II RSN to reach 6 cm peak flux density, the higher its 6 cm luminosity at that peak.

Unfortunately, there are only four Type Ib/c RSNe and 11 Type II SNe on which the relation can be tested. Even more unfortunate, the four Type Ib/c SNe are diverse, with two being Type Ib and two being Type Ic.

Within these limitations, however, examination of Fig. 5 implies that Type Ib/c SNe may be approximate radio standard candles having an average peak 6 cm luminosity of $L_{6\mathrm{cm\ peak}} \sim 10^{27}$ erg s^{-1} Hz^{-1} and Type II SNe may obey a relation for their peak 6 cm luminosity of $L_{6\mathrm{cm\ peak}} \sim 3 \times 10^{23}$ $(t_{6\mathrm{cm\ peak}} - t_0)^{1.5}$ erg s^{-1} Hz^{-1} with time in days. This relation is the solid line in Fig. 5.

10. Summary

Since the initial radio detection of SN1979C in April 1980, the past 17 years have yielded considerable information on RSNe. It appears that the radio emission can be used to estimate the presupernova mass loss rate and changes therein, to show the existence of filamentation in the presupernova stellar wind, and to indicate the possible presence of binary companions. More speculatively, radio observations may also provide a new technique for estimating distances.

Acknowledgments. KWW & MJM wish to thank the Office of Naval Research (ONR) for the 6.1 funding supporting this research.

References

Ball, L., Campbell-Wilson, D., Crawford, D. F., & Turtle, A. J. 1995, ApJ 453, 864

Brocato, E. & Castellani, V. 1993, ApJ 410, 99

Chevalier, R. A. 1982a, ApJ 259, 302

Chevalier, R. A. 1982b, ApJ 259, L85

Filippenko, A., Matheson, T., & Barth, A. 1994, AJ 108, 222

Gaensler, B. M., Manchester, R. N., Staveley-Smith, L., Tzioumis, A. K., Reynolds, J. E. & Kesteven, M. J. 1997, ApJ 479, 845

Lang, K. R. 1986, in *Astrophysical Formulae*, 47

Langer, N. & Maeder, A. 1995, A&A 295, 685

Montes, M. J., Weiler, K. W., & Panagia, N. 1997, ApJ, in press

Nomoto, K., Yamaoka, H., Pols, O. R., van den Heuvel, E., Iwamoto, K., Kumagai, S., & Shigeyama, T. 1994, Nature 371, 227

Podsiadlowski, Ph., Hsu, J., Joss, P., & Ross, R. 1993, Nature 364, 509

Ryder, S., Staveley-Smith, L., Dopita, M., Petre, R., Colbert, E., Malin, D., & Schlegel, E. 1993, ApJ 417, 167

Spyromilio, J. 1994, MNRAS 266, 61

Turtle, A. J., Campbell-Wilson, D., Bunton, J. D., Jauncey, D. L., Kesteven, M. J., Manchester, R. N., Norris, R. P., Storey, M. C., & Reynolds, J. E. 1987, Nature 327, 38

Van Dyk, S., Sramek, R. A., Weiler, K., & Panagia, N. 1993, ApJ 419, L69

Van Dyk, S., Weiler, K., Sramek, R., Rupen, M., & Panagia, N. 1994, ApJ 432, L115

Weiler, K., Sramek, R., Panagia, N., van der Hulst, J., & Salvati, M. 1986, ApJ 301, 790

Weiler, K., Panagia, N., & Sramek, R. 1990, ApJ 364, 611

Weiler, K., Van Dyk, S., Panagia, N., Sramek, R., & Discenna, J. 1991, ApJ 380, 161

Weiler, K., Van Dyk, S., Pringle, J., & Panagia, N. 1992a ApJ 399, 672

Weiler, K., Van Dyk, S., Panagia, N., & Sramek, R. 1992b ApJ 398, 248